

Synthesis of monodisperse CeO₂-ZrO₂ particles exhibiting cyclic superelasticity over hundreds of cycles

Zehui Du¹, Pengcheng Ye¹, Xiaomei Zeng¹, Christopher A Schuh³, Nobumichi Tamura⁴, Chee Lip Gan^{1,2*}

Dr.Zehui Du, Pengcheng Ye, Xiaomei Zeng, Prof. Chee Lip Gan*

1. Temasek Laboratories, Nanyang Technological University, 637553, Singapore

* Corresponding author: Chee Lip Gan, CLGan@ntu.edu.sg,

Prof.Chee Lip Gan

2. School of Materials Science and Engineering, Nanyang Technological University, 639798, Singapore

Prof. Christopher A Schuh

3Department of Materials Science and Engineering, Massachusetts Institute of Technology, Cambridge, MA 02139, USA

Dr. Nobumichi Tamura

4. Advanced Light Source (ALS), Lawrence Berkeley National Laboratory (LBNL), Berkeley, California, 94720, USA

Keywords: CeO₂-ZrO₂, particles, sol-gel, shape memory, superelasticity

* Corresponding author: Chee Lip Gan, CLGan@ntu.edu.sg

* Zehui Du and Pengcheng Ye contributed equally to this article

Abstract

Nano/micro scale CeO₂-ZrO₂ (CZ) shape memory ceramics are promising materials for smart micro electro-mechanical systems (MEMS) applications such as sensing, actuation and energy damping devices. However the processing method to mass produce such small volume ceramics particles has not yet been established. Herein, we reported a modified sol-gel method to synthesize highly monodisperse CeO₂-ZrO₂ (CZ) spherical particles with diameters in the range of 0.5 to 6 μm. Synchrotron X-ray micro-diffraction (μSXRD) confirmed that most of the particles are single crystals after annealing at 1450°C. The single crystalline particles exhibited significantly enhanced shape memory and superelastic properties with recoverable strain of up to ~4.7%. Highly reproducible superelasticity over more than five hundreds cycles and dissipated energies of up to ~40 MJ/m³ (per cycle) can be achieved in the 16 mol% ceria doped CZ particles. The cycling capability is enhanced ten times compared with our first demonstration (only 50 cycles in *Lai et.al, Science, 2013, 341, 1505*). Furthermore, the effects of cycling and testing temperature (in 25-400°C) on superelasticity have been investigated. Our work provides an approach to mass produce the small volume shape memory ceramics and paves a way for their engineering applications.

Introduction

Ceria stabilized tetragonal zirconia polycrystals ($x\text{CeO}_2-(1-x)\text{ZrO}_2$) are an important group of shape memory ceramics¹ with many potential applications in sensing, actuation and mechanical energy damping systems.^{2,3,4,5} These ceramics have been reported to exhibit very limited shape memory effect and superelasticity since it was first studied in bulk materials in the 1980s: the macroscopic stress-induced transformation strain in bulk samples was reported to be very small, only ~0.5-1.0% and the martensitic transformation underlying shape memory and superelastic properties could only be cycled a few times before intergranular cracking would compromise the sample.^{6,7} In contrast, our recent work^{8,9,10} has shown that single crystal or oligocrystalline micro- or nano-pillars of ceria doped zirconia can alleviate the cracking problem, as such structures relax the martensitic-transformation-induced mismatch stresses. The micro- or nano-pillars in those works exhibited significantly enhanced superelastic cycling capabilities (up to 50 cycles) and large shape memory strains of several percent.

However, for practical engineering applications, the superelastic behavior of the ceramics must be reproducible over hundreds or even thousands of cycles, in order to be functionally reliable when it is integrated into devices or systems. Furthermore, it is important to explore other manufacturing routes that have mass production and engineering application potentials and establish the processing method to synthesize such kind of small volume ceramics with highly cyclic superelasticity properties. As the key to the enhanced shape memory and superelasticity in zirconia ceramics appears to be fine scale, oligocrystalline or single crystal structures, one of the promising candidates is monodisperse nano or microparticles with spherical shape. Since the particles are in small volume, it can be easily crystallized into single crystals or oligocrystal by annealing. Moreover, such particles can be uniformly and closely packed into bulk powder

compacts, or even ordered colloidal crystals, retaining their large free surface area and yet enabling superelastic properties through a larger volume. What is more, monodisperse zirconia microspheres can be synthesized by a sol-gel processing method in which zirconium alkoxides are hydrolyzed and condensed in an alcoholic solvent using a small amount of water and catalyst.^{11,12,13} For example, Lerot et al. have synthesized zirconia microspheres by hydrolysis of zirconium tetra-n-propoxide in propanol, in the presence of long-chain carboxylic acids such as caproic acid, decanoic acid and eicosanoic acid as catalysts, obtaining particles with average sizes of ~0.1- 2.5 μm .¹⁴ Yan et al. have attained particle sizes of 0.8-4.0 μm through hydrolysis of zirconium propoxide in butanol with stearic acid.¹⁵ Van Canfort et al. have used 2-methoxyethanol (2-MOE) and decanoic acid as the solvent and the catalyst, respectively.¹⁶

Although the hydrolysis kinetics of the zirconium alkoxide as well as the resultant zirconia particle size appear strongly dependent on the concentration of water and the carboxylic acids, the interplay between these variables remains unclear. A comprehensive mapping of these parameters into a diagram would be a very useful guideline for the synthesis of zirconia microspheres for various fundamental studies and engineering applications. More urgently, the studies described above only address undoped zirconia microspheres produced by the sol-gel method, whereas superelasticity and shape memory require substantial doping to bring the tetragonal/monoclinic martensitic transformation temperatures into a suitable range (e.g., to room temperature).^{17,18}

It is our goal in this work to address these challenges, by developing a modified sol-gel processing method to produce ceria-doped zirconia microspheres, and to do so with an eye towards shape memory and superelastic properties. Our approach is based on the hydrolysis of zirconium tetrabutoxide ($\text{Zr}(\text{oBu})_4$) and cerium (IV) methoxyethoxide (CeOEM) in 2-MOE with decanoic acid as catalyst. Monodisperse CeO_2 - ZrO_2 microspheres with diameters varying in ~0.5-6 μm have

been synthesized for the first time and the binary water-acid diagram with the aim to enhance particle production has been established. The particles after sintering have been screened by μ SXRD and scanning electron microscope (SEM). On those single-crystal particles with perfect microstructure, we have further explored the shape memory effect and superelasticity properties at both room temperature and elevated temperatures up to 400°C by *in-situ* nanocompression. We successfully demonstrated unprecedented highly cyclic superelastic properties with large energy dissipation in the particles.

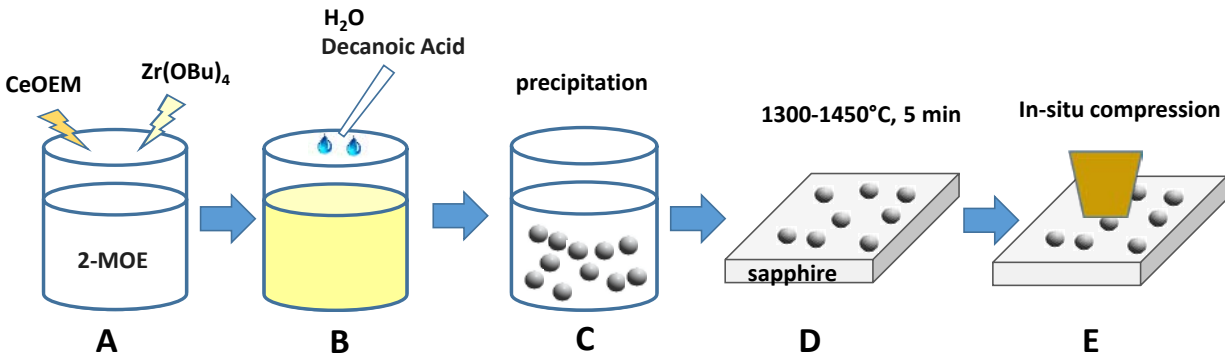


Figure 1 Schematic illustration of the synthesis processes for the monodisperse CZ microspheres and the setup for in-situ compression tests

Our synthesis process for monodisperse CeO₂-ZrO₂ (CZ) microspheres are schematically illustrated in Figure 1A-D. Zirconium tetrabutoxide (Zr(OBu)₄, C₁₆H₃₆O₄Zr) and cerium (IV) methoxyethoxide (CeOEM, Ce(OC₂H₄OCH₃)) were first mixed in 2-MOE. After vigorously stirring for 1 hour, decanoic acid and water were added into the mixture sequentially. Precipitation of the CZ microspheres took place after about 10 seconds. The CZ microspheres were then extracted and drop-cast on c-cut sapphire (0001) substrates. The microspheres were then annealed to form single crystal or oligocrystalline structures. Particles characterizations were performed by SEM, powder XRD and μ SXRD. Mechanical testing was conducted through instrumented

nanocompression using a flat diamond punch in an *in-situ* nanoindenter PI 85 or PI87 from Hysitron (Figure 1E). Experimental details are given in the Experimental Section.

Effect of acid/ water ratio on the particle sizes

Figure 2 shows the CZ microspheres prepared with various molar concentrations of water and decanoic acid. Monodisperse CZ microspheres are obtained when the acid concentration is 0.065M and the water concentration is in the range of \sim 0.7-1.5M (Figure 2A-D). Figure 3A shows the average particle sizes measured using ImageJ software¹⁹ as a function of the water concentration; these decline monotonically from \sim 2 to 0.8 μ m when the water concentration was increased from 0.7 to 1.5 M. The coefficient of variation over this range increase only slightly from \sim 5 to \sim 9%, reflecting a tight size distribution of highly monodisperse spheres. Figure 3B reveals the effect of acid concentration on the particle sizes at constant water concentration of 1.0M; it has little effect at lower concentrations, but leads to loss of monodispersity above about 0.075M, where the average diameter also drops to \sim 0.8 μ m. This significant change in the particle size distribution as a function of the acid concentration can be clearly observed in Figure 2C, E and F.

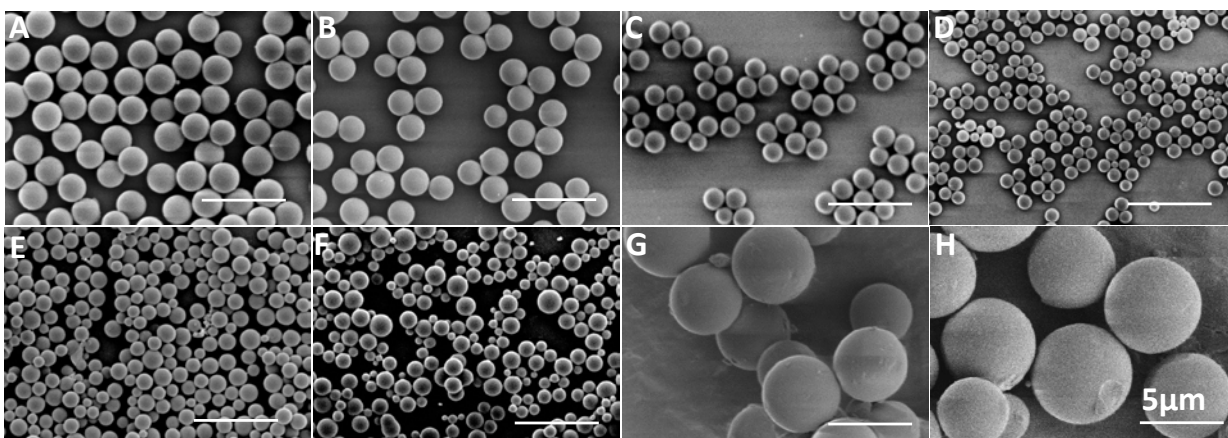


Figure 2 SEM images of CZ microspheres with different water and acid concentrations. [water]/[acid]: (A)0.7 M/ 0.065 M; (B) 0.85 M/0.065 M; (C)1.0 M/0.065 M; (D)1.5 M/0.065 M; (E)1.0 M/0.08 M; (F)1.0 M/0.1 M; (G)0.5 M/0.075 M; (H)0.5 M/0.085M. The Ce mol% is kept at 16 mol% and the samples were dried at 80 °C before SEM.

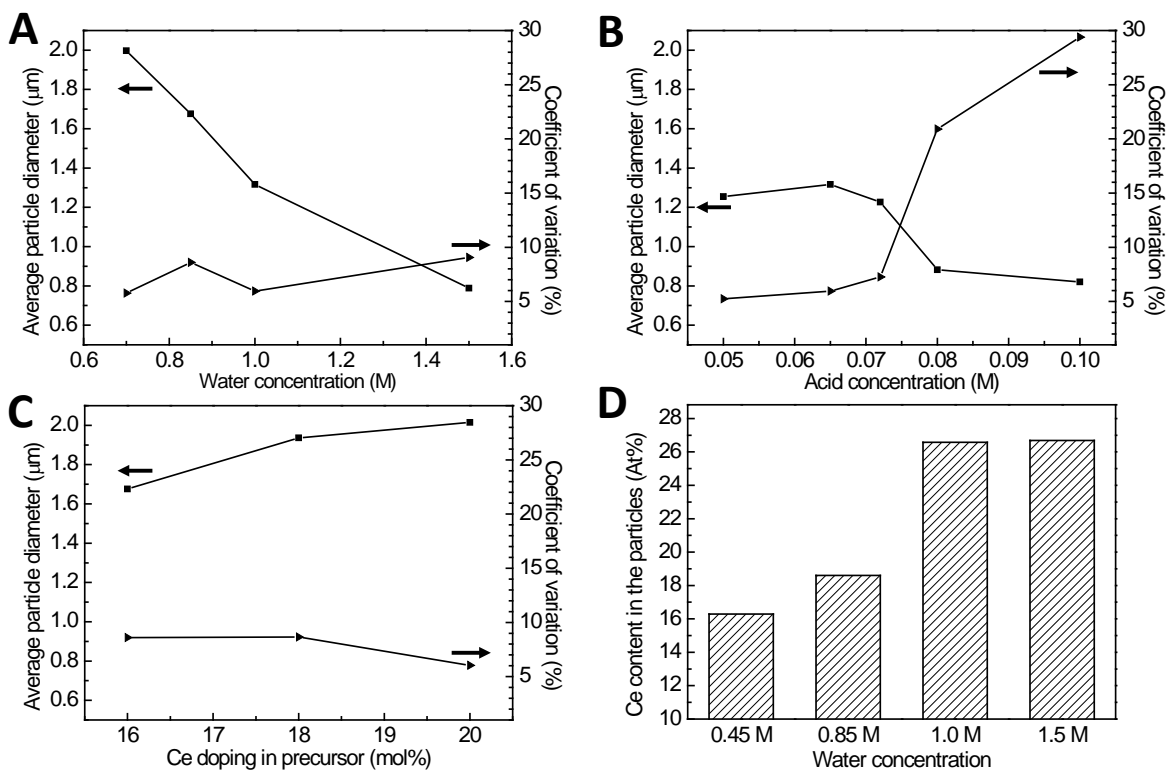


Figure 3 (A-C) The plots of average particle diameter and coefficient of variation (CV) of the CZ particles with different concentrations of water ([acid]=0.065M) (A), decanoic acid ([water]=1.0M) (B) and cerium precursor ([water]/[acid]=0.85M/0.065M) (C); (D) atomic percentage of cerium in the CZ particles after drying ([acid]=[0.065] and initial Ce addition= 16%)

It is possible to obtain CZ microspheres with diameters as large as 4-6 μm by reducing the water concentration to 0.5M, as shown in Figure 2G-H, but their sizes have high coefficients of variation and must be considered polydispersed. When the water concentration is 0.4M or lower, no precipitation was observed and the solution cured into a transparent gel. Based on the water and acid concentrations we have studied, a water-acid diagram for mapping the correlations between the average particle size and the water and acid concentration can be established, as shown in Figure 4.

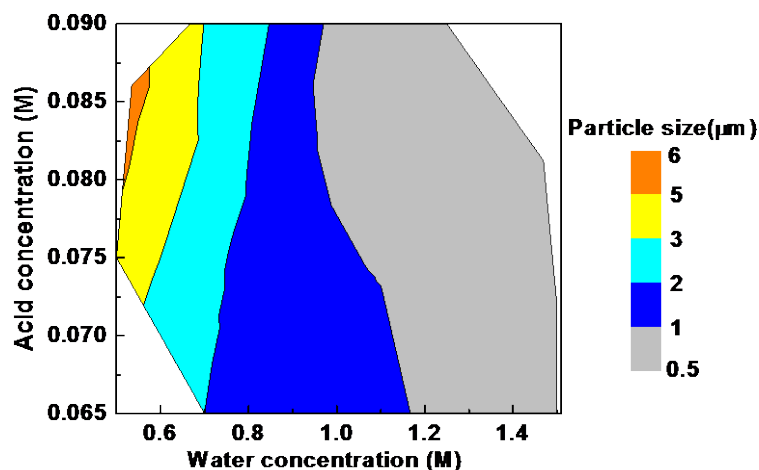


Figure 4 A water-acid diagram mapping the average particle size vs. acid and water concentrations. Ce mol%=16%.

To prepare particles with ceria doping concentration from 16 to 20 mol%, the molar concentration of the cerium precursor in the solution was changed over the range 0.016 to 0.02M. In addition to changing the doping level in the particles, we observed that the average diameter of the resultant CZ microspheres slightly increased from 1.7 to 2.0 μm with ceria addition, while the particles remained monodispersed (Figure 3D). This increase of particle size can be attributed to the formation of bimetallic complexes from zirconium tetrabutoxide and cerium methoxyethoxide through ligand exchanges.²⁰ As bimetallic complexes have higher stability than the corresponding single metal alkoxides, hydrolysis will be slowed down, as has been evidenced in our experiments. We observed that the induction time preceding precipitation doubled from ~ 30 seconds to about one minute with the increase in the concentration of cerium precursor; this supports an interpretation that the hydrolysis reaction was retarded. With fewer nuclei formed in the first burst, more matter is available for growth, resulting in larger particles.

We have used energy-dispersive X-ray spectroscopy (EDS) to semi-quantitatively measure the elementary compositions of the CZ microspheres prepared by adding cerium precursors at a 16 mol% level. As shown in Figure 3D, the actual cerium concentration incorporated in the CZ

particles is very sensitive to the water level. At 0.45-0.85 M water, the incorporated cerium concentration is ~16-18 mol%, close to the initial addition level. When the water addition increased to 1.0-1.5M, the cerium concentration increased monotonically to ~26 mol%, and the typically light yellow color of the particles became darkened.

Crystallization of the particles

The CZ microspheres prepared by the sol-gel method are amorphous, and are therefore subsequently annealed at 700-1450°C in order to obtain single crystal or oligocrystal particles for studies of their shape memory and superelastic properties. SEM images of the particles after annealing are shown in Figure 5A-D. The particles annealed at 700°C are nanocrystalline with a grain size less than 50 nm. With increasing annealing temperature from 700 to 1400°C, the grain size increases and the grain boundaries become thermally etched. At 1400°C, the particles are polycrystalline with a grain size of ~200-500nm. The grain boundaries disappear at 1450°C, and the prominence of crystallographic faceting suggests that a single crystalline state has been achieved.

X-ray powder diffraction measurements on these annealed samples show that the crystals are in the tetragonal phase, and bear no special orientation relationship with the (0001) sapphire substrate (Figure S1 in Supplementary Materials). To study the sample crystallography at the particle level, synchrotron radiation scanning X-ray micro-diffraction (μ SXRD) has been carried out using a white beam. Figure 5E shows a SEM image of a typical area containing six single particles or particle clusters, labelled as #1-6. Figure 5F shows the corresponding Laue diffraction orientation map in which each color represents one crystal orientation. It reveals that each isolated particle has only one crystal orientation (e.g. #1, #2 and #3), i.e., these particles are single crystalline. Particle clusters, on the other hand, shows 2-3 crystal orientations, for example #4-6.

A representative Laue diffraction pattern from particle #3 is shown in Figure 5G, and indexed as tetragonal zirconia with a specific crystal orientation (indexed spots are marked by squares). The unindexed diffraction spots are associated with the sapphire substrate (c.f. Figure S2). Similar μ SXRD analysis has been carried out on several other areas of the sample, generally confirming that the majority of the particles are single crystals, especially those that appear free of grain boundaries by SEM.

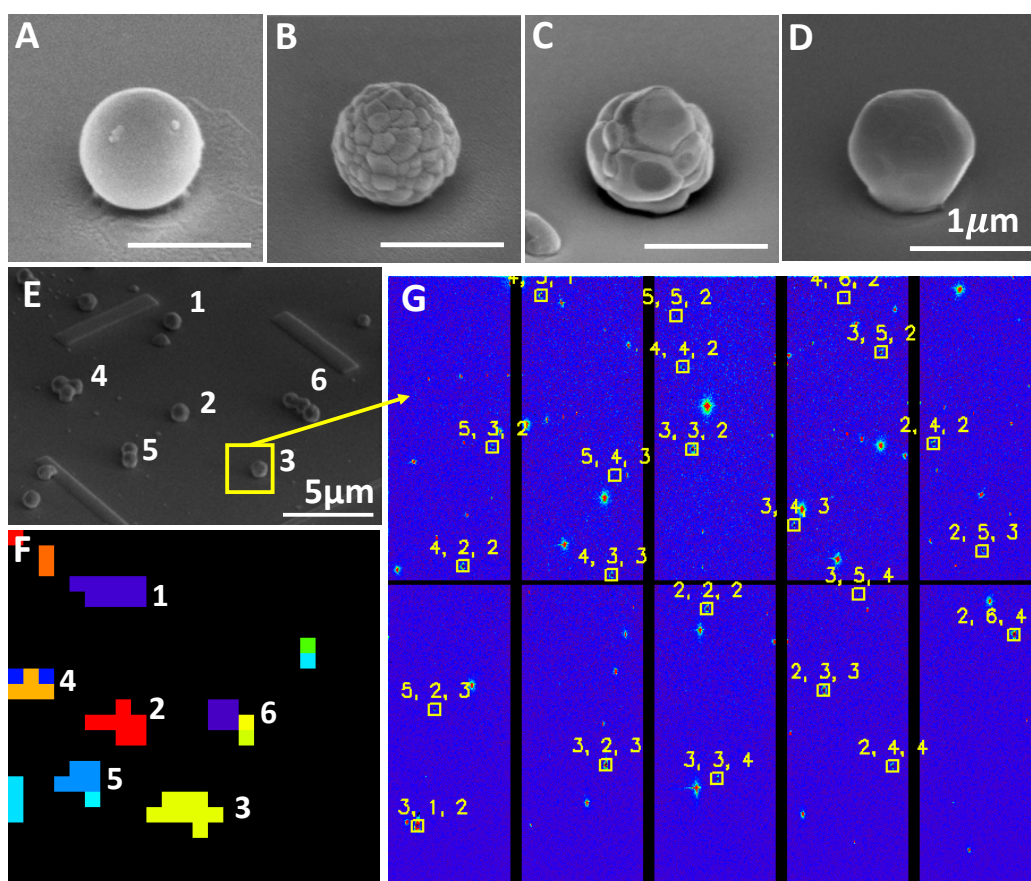


Figure 5 SEM images of the CZ particles after annealing at (A) 700°C for 30 mins; (B) 1300 °C for 5mins; (C) 1400 °C for 5mins; and (D) 1450 °C for 5mins. (E) SEM image of a few particles on sapphire substrate; (F) the orientation map of the particles corresponding with (E); (G) white beam microdiffraction pattern of Particle #3 in (E); The particles were prepared using $[\text{water}]/[\text{acid}]=0.85\text{M}/0.065\text{M}$ and with 16 mol% ceria doping.

Shape memory and superelastic properties of the particles

The shape memory and superelastic properties of the CZ particles annealed at 1450°C have been studied by *in-situ* nanocompression in an SEM. Two types of single crystal particles doped with 14 and 16 mol% Ce respectively have been chosen for these studies.

Particle #7 provides an example of superelastic properties. This particle is doped with 16 mol% Ce, has a diameter of 0.94 μm , and a crystal orientation close to (111), in the direction of the compression axis. Figure 6A shows the load-displacement curve obtained by applying a maximum compressive load of 750 μN at a loading rate of 50 $\mu\text{N/s}$. After an initial elastic deflection, a single large displacement plateau spanning $\sim 18\text{nm}$ is observed at a load of $\sim 620 \mu\text{N}$. This plateau is attributable to the stress-induced martensitic transformation²¹, and corresponds to a relative particle distortion, or transformation “strain” ($\varepsilon_{a \rightarrow m}$)^{22,23}:

$$\varepsilon_{a \rightarrow m} = \frac{d_{a \rightarrow m}}{2R} \quad (1)$$

where $d_{a \rightarrow m}$ is the total displacement in the displacement plateau and R is the radius of particle. Therefore the transformation strain of particle #7 is $\sim 1.91\%$. That the 1.91% strain is a result of the transformation is supported by its perfect recovery during unloading, with another displacement plateau at 170 μN corresponding to the reverse martensitic transformation. The sample hence exhibits the essential characteristics of the superelastic effect.²⁴ Based on the load-displacement curves, the dissipated energy for one superelastic cycle of particle #7 is estimated to be $\sim 25.2 \text{ MJ/m}^3$.

This superelastic deformation and shape recovery has been observed in real-time by *in-situ* SEM during the testing (video can be provided upon request). What is more, we have applied over five hundreds cycles of compression on this particle at the same fixed load of 750 μN , as shown

in Figure S3 of the Supplementary Materials. Figure 6B-C shows the particle before the first compression and after compression through 502 cycles; the particle is almost intact and shows no major change in its shape. A more detailed discussion on the effect of cyclic superelasticity will be made in the next section.

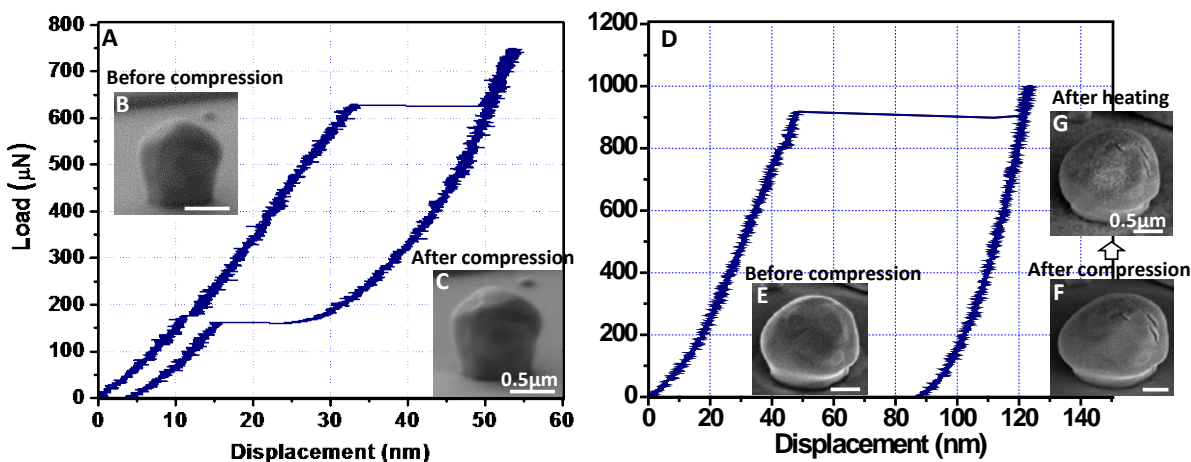


Figure 6 Load-displacement curves of the CZ particles (A) #7, with 16% cerium doping; (B) #8, with 14% cerium doping (Ce mol% was confirmed by EDX). The particles were sintered on c-cut sapphire substrate at 1450°C for 5 minutes. Tiny cracks observed in (F and G) are presented in the platinum (Pt) coating of the CZ particle. The Pt was coated for SEM imaging.

Particle #8 is doped by 14 mol% Ce and has a diameter of $\sim 1.64\mu\text{m}$. It exhibited a very typical load-displacement curve for a shape memory material below the reversion temperature; as shown in Figure 6D, it experienced a sudden displacement plateau spanning 77nm at $\sim 916\mu\text{N}$ corresponding to the forward martensitic transformation, but it did not recover this strain upon unloading. The transformation induced strain is estimated to be $\sim 4.7\%$ in this case. By comparing the SEM images of the particle before and after compression (Figure 6 E-F), the shape change appears evident. The observed small cracks at the surface of the particle after cyclic compressions are in the Pt coating used for SEM imaging, not in the particle. The fact that most of the shape change can be attributed to the martensitic transformation is revealed by heating it through the

reverse transformation; after 1 hour at 500°C (c.f. Figure 6E and G) the particle shape resembles its uncompressed form.

We have tested dozens of particles with different sizes and cerium doping concentrations. In general, most of the particles exhibited robust shape memory or superelastic properties depending on the cerium doping concentration, while a minority of them did not. This phenomena are apparently associated with the crystal orientation of the particles as some crystal orientations favour martensitic transformation, while some favour planar slip or fracture before transformation.¹⁰ The concentration of stresses between transformed and untransformed regions within a single particle due to the Hertzian contact geometry of the particles and nanoindentation tip could be another reason for the failure²⁵. Nevertheless, we have successfully synthesized monodisperse CZ particles with significantly enhanced superelasticity and shape memory properties by a modified sol-gel processing method. The shape memory strain up to ~4.7%, highly reproducible superelasticity with cycling over five hundreds times and dissipated energy of ~25.2 MJ/m³ (some particles can reach ~40 MJ/m³ in) can be achieved. The cycling capability is enhanced ten times compared with our first demonstration in which only 50 cycles were possible⁸. The improvement in the superelastic cycling can be attributed to the single crystalline nature of the particles at nano/micro scales as such particles have few structural flaw that induces cracks and the large free surface area can alleviate the mismatch transformation stress to the largest extent.

Superelastic cycling of the particles

The effect of cycling on the superelasticity has been studied on the particles with diameter of ~0.85 μm and doped by 16 mol% of Ce. Figure 7A-B shows a series of load-displacement curves of a representative particle (#9) for the 1st-412th cycles of compression. On the 1st cycle, the forward transformation occurs through two to three displacement plateaus in the loading curve. In

the unloading curve, there are also a few steps in the displacement plateau associated with the reverse martensitic transformation. Over the subsequent 6-14 cycles we observe a shakedown in the superelastic curves as the particle adopts its favored kinematic transformation pathway, and also accommodates the shape constraints of the platens (note the initial unrecovered strains in these early cycles, which are eventually shaken out as the cycles become fully reversible).

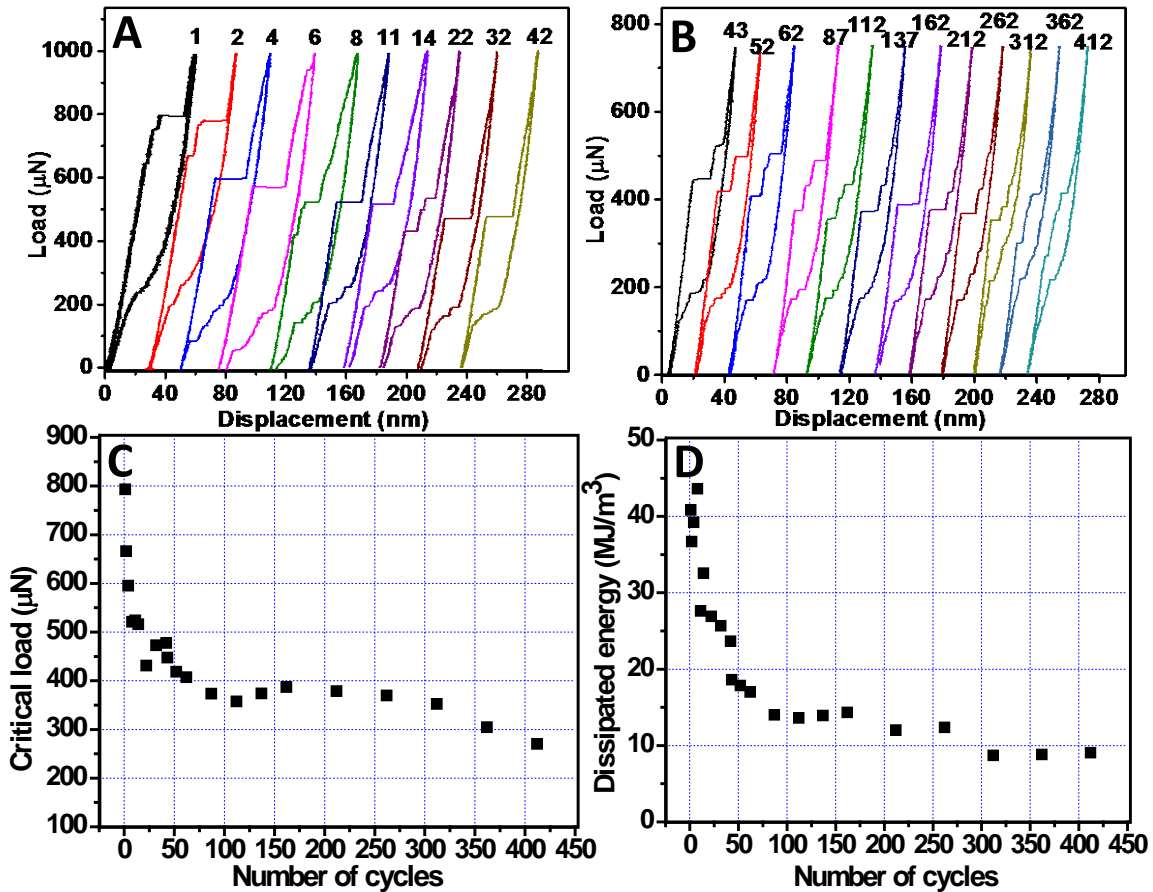


Figure 7 Load-displacement curves of the CZ particle 9# under (A) 1-42th cycles and (B) 43-412th cycles of compression; (C) the critical load and (D) the dissipated energy of the particle under different superelastic cycles. The particles were with 16 mol% Ce and sintered on c-cut sapphire substrate at 1450°C for 5 minutes.

From the 2nd to 87th cycles, similar displacement plateaus are found in each loading-unloading curve, with a slight training effect stabilizing the preferred configuration of martensite; after such stabilization the superelastic cycles became reasonably superimposable, for example, the 87th - 262th cycles in Figure 7B. We stopped the loading of this particle after the 412th cycle although it showed no sign of failure at that point.

One interesting observation in Figure 7A-B is that the critical load for inducing martensitic transformation (austenite → martensite) decreased with continued cycling of the applied load, as has been summarized in Figure 7C. This decreasing tendency is more pronounced in the first 100 cycles during the shakedown period. It decreased from ~793 to ~360 μN between the 1st and 100th cycle. A similar cycling shakedown effect has been reported in fine-grain Ni-Ti shape memory alloy (SMA), Cu-Zn-Al SMA microwires²⁶ and Cu-Al-Ni micropillars²⁷, and can be attributed to the development of dislocation substructure which accommodates the martensite plates in the austenite matrix.^{28,29} As a consequence, martensite domains can evolve at lower stresses in the subsequent loading cycles. The critical load becomes almost constant in the 100th -300th cycle, probably due to the stabilization of martensitic transformation path. Similar trends are reflected in the energy dissipated on each cycle, i.e., the area inside the superelastic loop, which is shown in Figure 7D. Nevertheless, the dissipated energy in the first ten cycles is very high, averaging in ~40 MJ/m³ and it slightly dropped to ~ 20-30 MJ/m³ in the subsequent 10th-40th cycles. The dissipated energy is higher than that achieved in many shape memory alloys such as Ni-Ti, Cu-Al-Mn-Ni and Ni-Ti-Nb alloys (10 - 20 MJ/m³).^{30,31,32}

High temperature superelasticity

A series of CZ particles of diameter 0.92 μm was also tested using the *in-situ* nanoindenter PI 87 (Hysitron) equipped with a MEMs heater, to explore the role of ambient temperature on the

transformation properties. The particles were compressed at three different temperatures, namely 25, 200 and 400°C, sequentially and for only five loading cycles at each temperature. Figure 8A shows the load-displacement curves at 25°C. The curves are typical superelastic loops, and after one cycle for platen accommodation the displacement becomes fully recoverable after the 2nd cycle, and the curves are highly repeatable. The load-displacement curves of the 2nd cycle of compression at each of 25, 200 and 400°C are plotted in Figure 8B for comparison. The curves are very similar except that the critical loads for martensitic transformation and the area enclosed in the hysteresis loops are changed. The critical load gradually increases with temperature (Figure 8C), which is expected as the austenite phase (i.e. tetragonal phase for zirconia) is more stable at high temperatures and thus higher stress is required for the stress-induced martensitic transformation.³³ Figure 8D reveals that the dissipated energy in each superelastic cycle decreased with increasing testing temperatures, owing to a reduction in the transformation strain, as shown in Figure 8B. Nevertheless, these observations are the first we are aware of to show that superelasticity can be retained in CZ at elevated temperatures up to 400°C. It indicates that the as-developed CZ particles have the potentials to be used for energy damping or actuation in high-temperature environments.

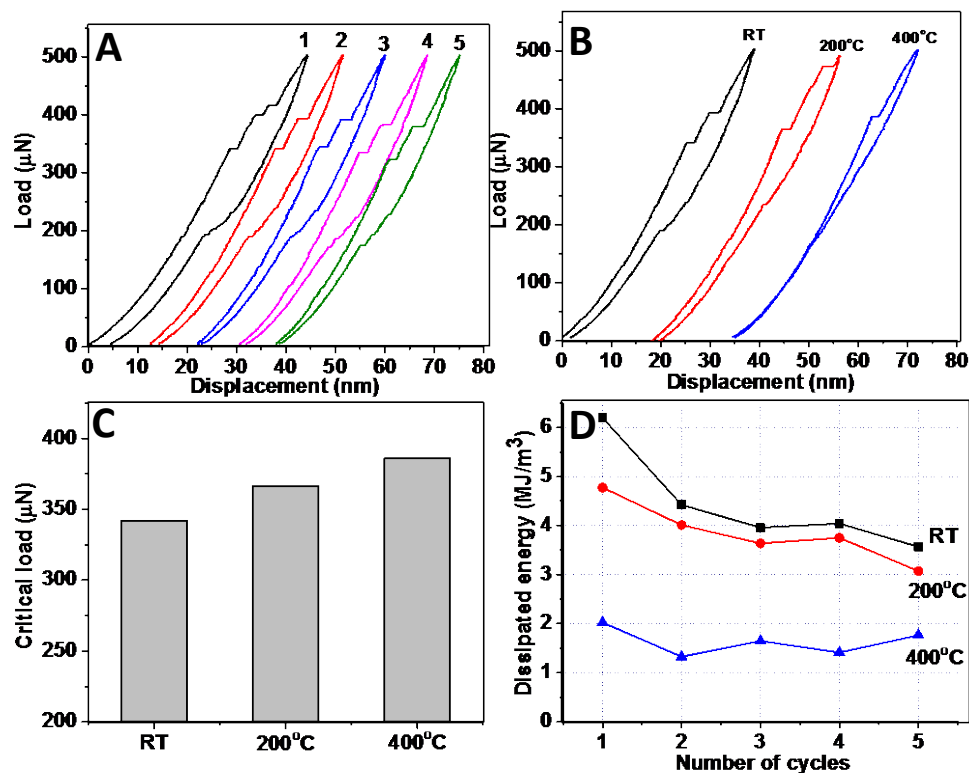


Figure 8 Load-displacement curves of a superelastic CZ particle #10 under (A) 1-5th cycles of compression at room temperature (RT) and (B) 2nd cycle at 25°C, 200°C and 400°C ; (C) the critical load and (D) the dissipated energy of the particle tested at different temperatures. The particles were with 16 mol% Ce and sintered on c-cut sapphire substrate at 1450°C for 5 minutes.

Conclusion

Monodisperse ceria-doped zirconia (CZ) microspheres have been produced by a modified sol-gel processing method, for which we empirically optimized the concentrations of water, decanoic acid and cerium precursors. Monodisperse CZ microspheres with diameters of 0.8-2.0 μm are obtained for acid concentrations lower than 0.075M and water concentrations in the range of 0.5-1.5M. The particle size rises with a decreasing water addition. Larger microspheres with diameters of 4.0-6.0 μm can be obtained by using 0.5M water and 0.075-0.085M acid, although these conditions lead to greater polydispersity. The particle size is also increased by increasing the

concentration of cerium precursor. Upon annealing at 1450°C, we obtain mostly single crystal particles suitable for superelastic and shape memory testing.

The CZ single crystal particles exhibited excellent shape memory and superelastic properties with transformation induced strains up to 4.7%. At 16 mol% ceria doping, CZ particles exhibited highly reproducible superelasticity through over 500 load cycles, with dissipated energy up to ~40 MJ/m³ per cycle. Superelasticity was also observed directly in-situ during microcompression, and is attributed to the reversible martensitic transformation. Upon cycling, we observe gradual accommodation of the platen geometry, as well as a shakedown in critical load and dissipated energy of the particle. At temperatures above ambient, the transformation requires higher stresses to trigger, but superelastic properties are retained to at least 400°C.

Supporting Information

Supporting Information is available from the Wiley Online Library or from the author.

Figures S1-S3

Acknowledgments

We would like to thank Joseph Lefebvre, Ryan J. Stromberg and Ariel Leonard from Hysitron. Inc. for their kind help with high temperature in-situ indentation at Hysitron in Minnesota, USA. The Advanced Light Source (ALS) and the National Energy Research Scientific Computing Center (NERSC) are supported by the Director, Office of Science, Office of Basic Energy Sciences, of the U.S. Department of Energy under Contract No. DE-AC02-05CH11231 at the Lawrence Berkeley National Laboratory (LBNL).

Experimental

Materials

All of the chemicals used in the experiments were analytical grade and were used without further purification. zirconium tetrabutoxide (80% in butanol), 2-methoxyethanol and decanoic acid were purchased from Sigma-Aldrich. Cerium (IV) methoxyethoxide (18-20% in methoxyethanol) was purchased from Gulf Chemical.

Synthesis of Monodisperse Spherical CZ Particles and Characterization

To synthesize the zirconia particles with 16-20 mol% ceria doping, zirconium tetrabutoxide (80% in butanol) and cerium (IV) methoxyethoxide (18-20% in methoxyethanol) were firstly added to 2-methoxyethanol (2-MOE) according to the molar ratios of Ce:Zr in the desirable particles. The total concentration of cerium and zirconium alkoxides in 2-MOE is kept at 0.1M. The mixture was kept stirring for one hour. Then decanoic acid was added to the mixture. After stirring for 1 hour, water was dropped into the mixture. It takes about 10 seconds before precipitation occurred. The solution was then aged for two hours. All the steps described above were carried out in a glove box filled with Argon and the relative humidity inside the glove box was kept at ~22%. In order to study the effect of water and decanoic acid concentration on the particle size, water concentration was varied in ~0.40 M-1.5 M and acid concentration was in ~0.05 M-0.1 M.

After aging, CZ particles was extracted from the suspension solutions by centrifuging at 3500 rpm for 3 mins and washed by 2-MOE. The process of centrifugation and washing was repeated for three times. Finally the washed particles were dispersed in 2-MOE and dropped on glass slides for imaging. The morphology and chemical composition of the CZ particles were analyzed by field emission scanning electron microscope (FESEM, FEI Nova 600i Nanolab, 5-15

kV) equipped with energy-dispersive X-ray spectroscopy (EDS). The particle size was analyzed with image analysis software (ImageJ, National Institutes of Health, West Bethesda, MD).¹⁹

Annealing of the CZ Particles and Characterization

The as-prepared particles were firstly dispersed in 2-MOE and then dropped on sapphire (0001) substrate. After drying, the samples were annealed in a box furnace at 700°C for 30 mins, or 1300 °C, 1400 °C and 1450 °C for 5 mins and the ramping rate was kept at 10-20 °C/min. The crystallization of the particles was analyzed by X-ray diffraction (D8, Bruker) with Cu K α radiation. The crystal structure of some individual particles was studied by synchrotron radiation scanning X-ray micro-diffraction (μ SXRD) technique using a white beam on Beamline 12.3.2³⁴ at the Advanced Light Source, Berkeley, CA. The μ XRD patterns were collected in 1 second at a step size of 1 μ m for each frame by a DECTRIS Pilatus hybrid pixel array detector and analyzed using the XMAS (μ XRD analysis software) software package.^{35,36}

Micro-compression tests on the CZ particles

Micro-compression tests on the CZ particles (14 mol% or 16 mol% ceria) have been carried out on an in-situ nanoindenter (PI85, Hysitron) equipped with a 60° conical tip with a flat end (diameter: 5 μ m). The tip was carefully aligned on the particles by using SEM imaging. The loads applied were in the range of ~500-1500 μ N and the loading rate was ~50 μ N/s. To perform over hundreds of cycles of tests in a reproducible and comparable way, we separated the tests into ~40-50 segments in which 10 identical loading & unloading cycles were conducted with the specified maximum load and constant loading rate. Between the segments, a set-point 2 μ N contact force was always maintained and the contact with specimen was never broken. Based on the load-displacement curves, the dissipated energy each superelastic cycle can be evaluated. It is equal to

the area enclosed by the hysteresis loop in the load-displacement curves divided by the particle volume.

The CZ particles were also tested at elevated temperatures of 200°C and 400°C by in-situ nanoindenter PI87 (Hysitron, Minneapolis, MN) equipped with 1µm flat punch and a 400°C heating stage. The heating was controlled by a MEMs heater embedded with a thermocouple. Each testing was commenced after 20 minutes from the point that the targeted temperature has reached. The loads applied were in the range of ~500-750 µN and the loading rates are ~50 µN/s. Total five cycles of compression have been applied at each testing temperature, including 25°C, 200°C and 400°C.

References

- [1] K. E. Schurch, K. H. G. Ashbee, *Nature*, 1977, 266, 706
- [2] C. Chluba, W. Ge, R. L. Miranda, J. Strobel, L. Kienle, E. Quandt, M. Wuttig, *Science*, 2015, 348, 1004
- [3] L. Sun, W.M. Huang, Z. Ding, Y. Zhao, C.C. Wang, H.Purnawali, C. Tang, *Mater. Des.* 2012, 33, 577
- [4] I. Karaman, B. Basaran, H.E.Karaca, A.I. Karsilayan, Y.I. Chumlyakov, *Appl. Phys. Lett.* 90(2007) 172505:1-3.
- [5] A. Nespoli, D. Rigamonti, E.Villa, F. Passaretti, *Sens Actuators A Phys.* 218 (2014) 142–153.
- [6] P.E. Reyes-Morel, J.S. Cherny, I.W. Chen, *J. Am. Ceram. Soc.* 1988, 71, 648
- [7] P.E. Reyes-Morel, I.W. Chen, *J. Am. Ceram. Soc.* 1988, 71, 343
- [8] A. Lai, Z. Du, C.L. Gan, C.A. Schuh, *Science*, 2013, 341, 1505
- [9] Z. Du, X.M. Zeng, Q. Liu, A. Lai, S. Amini, A. Miserez, C.A. Schuh, C.L. Gan, *Scrip. Mater.* 2015, 101, 40
- [10] X.M. Zeng, A. Lai, C. L. Gan, C. A. Schuh, *Acta Mater.*, 2016, 116, 124–135
- [11] T. Ogihara, N. Mizutani, and M. Kato, *Ceram.Int.*, 1987, 13, 35.
- [12] J. Widoniak, S. Eiden-Assmann, and G. Maret, *Eur. J. Inorgan. Chem.*, 2005, 3149
- [13] H. Kumazawa, Y. Hori, and E. Sada, *Chem. Eng. J.*, 1993, 51, 129.

-
- [14] L. Lerot, F. Legrand, and P. De Bruycker, *J. Mater. Sci.*, 1991, 26, 2353.
- [15] B. Yan, C. V. McNeff, F. Chen, P. W. Carr, and A. V. McCormick, *J. Am. Ceram. Soc.*, 2001, 84, 1721.
- [16] O. Van Cantfort, B. Michaux, R. Pirard, J. P. Pirard, and A. J. Lecloux, *J. Sol-Gel Sci.Tech.*, 1997, 8, 207.
- [17] J. Yan, X. Li, S. Cheng, Y. Ke, X. Liang, *Chem. Commun.*, 2009, 2929–2931, 2929.
- [18] J. Widoniak, S. Eiden-Assmann, G. Maret, *Eur. J. Inorg. Chem.* 2005, 3149–3155
- [19] T. J. Collins, "ImageJ for microscopy," *Biotechniques*, vol. 43, pp. 25-30, 2007
- [20] N. Y. Turova, *The chemistry of metal alkoxides*: Boston : Kluwer Academic Publishers, 2002.
- [21] J.M.S. Juan, M.L. Nó, C.A. Schuh, *Adv. Mater.*, 2008, 20, 272.
- [22] J. Paul, S. Romeis, J. Tomas, W. Peukert, *Adv. Powder Tech.* 2014, 25, 136
- [23] K. Zheng, C. Wang, Y. Q. Cheng, Y. Yue, *Nature Comm.* 2010, 1021, 1
- [24] J.S. Juan, M.L. Nó, C.A. Schuh, *Nat. Nanotechnol.* 2009, 4, 415
- [25] Z. Du, X.M. Zeng, Q. Liu, C.A. Schuh, C.L. Gan, *Acta Mater*, in submission, 2016
- [26] S. M. Ueland, C.A. Schuh, *Acta Materialia*, 2012, 60, 282
- [27] J. S. Juan, M.L. Nó, C.A. Schuh, *Acta Materialia*, 2012, 60, 4093
- [28] T. Simon, A. Kroger, C. Somsen, A. Dlouhy, G. Eggeler, *Acta Materialia*. 2010, 58, 1850
- [29] A. Ibarra, D. Caillard, J. San Juan, M.L. No, *Appl. Phys. Lett.*, 2007, 90, 101907
- [30] Y. Tanaka, Y. Himuro, R. Kainuma, Y. Sutou, T. Omori, K. Ishida, *Science*, 2010, 327, 1488
- [31] V. Humbeeck, *Adv Eng Mater*, 2001, 3, 837
- [32] N.N. Sia, W.G. Guo, *Mech. Mater.*, 2006, 38, 463
- [33] K. Otsuka, C.M. Wayman, *Shape memory materials*, Cambridge University Press, 1998, P28.
- [34] N. Tamura, A.A. MacDowell, R. Spolenak, B.C. Valek, J.C. Bravman, W.L. Brown, R.S. Celestre, H.A. Padmore, B.W. Batterman, J.R. Patel, *J. Synchrotron Rad.*, 2003, 10, 137
- [35] N. Tamura *XMAS: A versatile tool for analyzing synchrotron X-ray microdiffraction data*. In: *Strain and dislocation gradients from diffraction* (Ice G. E. & Barabash R.) Imperial College Press, 2014, 125–155.

Synthesis of monodisperse CeO₂-ZrO₂ particles exhibiting cyclic superelasticity over hundreds of cycles

Authors: Zehui Du, Pengcheng Ye, Xiaomei Zeng, Christopher A Schuh, Nobumichi Tamura, Chee Lip Gan

Synopsis TOC

Highly monodisperse CeO₂-ZrO₂ (CZ) particles has been synthesized by a sol-gel method and exhibited excellent shape memory and highly reproducible superelastic properties with cycling over 500 times and the dissipated energy up to ~40 MJ/m³ (per cycle). The effects of cycling and testing temperature (in 25-400°C) on the superelasticity have been investigated.

